Pergamon

Stirring geochemistry in mantle convection models with stiff plates and slabs

Geoffrey F. Davies*

Research School of Earth Sciences, Australian National University, Canberra, ACT 0200, Australia

Abstract—Numerical models of mantle convection are presented that readily yield midocean ridge basalt (MORB) and oceanic island basalt (OIB) ages equaling or exceeding the apparent ~1.8-Ga lead isotopic ages of trace-element heterogeneities in the mantle. These models feature high-viscosity surface plates and subducting lithosphere, and higher viscosities in the lower mantle. The formation and subduction of oceanic crust are simulated by means of tracers that represent a basaltic component. The models are run at the full mantle Rayleigh number and take account of faster mantle overturning and deeper melting in the past. More than 97% of the mantle is processed in these models. Including the expected excess density of former oceanic crust readily accounts for the depletion of MORB source relative to OIB sources. A novel finding is of gravitational settling of dense tracers within the low-viscosity upper mantle, as well as at the base of the mantle. The models suggest as well that the seismological observation of a change in tomographic character in the deep mantle might be explained without the need to postulate a separate layer in the deep mantle. These results expand the range of models with the potential to reconcile geochemical and geophysical observations of the mantle. *Copyright © 2002 Elsevier Science Ltd*

1. INTRODUCTION

The persistence of isotopic heterogeneity in the convecting mantle, apparently for times approaching two billion years, has been a continuing source of puzzlement and debate. Because flow at the observed velocities of the surface tectonic plates would overturn the upper mantle within perhaps tens of millions of years and the whole mantle within a few hundred million years, it was presumed initially that some kind of compositional layering in the mantle was implied, to explain the much greater apparent ages of lead isotope heterogeneities in mantle-derived rocks (Jacobsen and Wasserburg, 1979). This has remained the most common presumption, especially as most attempts to model convective stirring of the mantle have failed to yield such persistence of heterogeneities, and in spite of the now-widespread acceptance that there is a considerable flux of material between the upper mantle and the lower mantle (Grand et al., 1997).

Many of the earlier attempts to quantitatively address this question assumed or implied constant-viscosity convection scaled to the upper mantle (e.g., Allegre and Turcotte, 1985; Hoffman and McKenzie, 1985), and these yielded survival times of heterogeneities of only a few hundred million years. On the other hand, models that were scaled to the whole mantle and that included some approximation to platelike surface behavior and an increase in viscosity with depth yielded longer survival times, approaching 2 Ga in a few cases (Gurnis and Davies, 1986a, b). However, the latter models were still idealized in important respects, and their results were more suggestive than compelling. Counterexamples were also presented and the debate continued (e.g., Kellogg and Turcotte, 1986, Kellogg and Turcotte, 1990; Christensen, 1989, Christensen, 1990; Davies, 1990a).

The interpretation of isotopic heterogeneity that predomi-

nated for a long time was that the lower mantle convected separately from the upper mantle and that the observed ancient heterogeneities were due to a small flux of material leaking from the lower mantle into the upper mantle (Jacobsen and Wasserburg, 1979; O'Nions and Tolstikhin, 1996). This view was finally abandoned by most people in the face of strong evidence from seismology that subducted lithosphere plunges deep into the lower mantle in several parts of the world (Grand, 1994; Grand et al., 1997; van der Hilst et al., 1997). This seismic evidence reinforced other arguments, which were based on seafloor topography, against a barrier to flow between the upper mantle and lower mantle (Davies, 1988; Davies and Richards, 1992).

Meanwhile, Hofmann and White (1982) had proposed that the isotopic heterogeneity observed in oceanic island basalts (OIBs) is derived from ancient oceanic crust that had been subducted and later returned to the surface in mantle plumes. They proposed that subducted crust settles to the bottom of the mantle because of its presumed greater density, and rises much later in mantle plumes, having been heated by the combined action of heat from the core and heat generated internally by the higher complement of radioactive heat sources carried by oceanic crust. They proposed that the resulting layer of segregated material was relatively thin, and might correspond to the seismic D″ layer at the base of the mantle. This proposal has survived well, both on geochemical and geophysical grounds (e.g., Davies, 1990b; Christensen and Hofmann, 1994; Hofmann, 1997; Coltice and Ricard, 1999) and for some time no one, to my knowledge, has argued against at least some role for gravitational settling and compositional stratification.

There have been many other studies of aspects of the mantle stirring problem, such as the effects of three dimensionality, spherical geometry, and toroidal flow, or addressing particular aspects of geochemical observations, such as degassing of the noble gases, which will not all be reviewed here. However, results that have some direct relevance to the present work are those of van Keken and Ballantine (1998), who showed that

there was essentially no difference between the degassing rates of the upper mantle and lower mantle as a result of the effect of higher viscosity in the lower mantle. Follow-up work has shown that this result is unchanged if account is taken of mantle phase transformations and a modest temperature dependence of viscosity (van Keken and Ballantine, 1999), or if heating through the base of the models is reduced from 60% to zero (Hunt and Kellogg, 2001).

It has been proposed that there might be a layer in the lowermost 1000 km of the mantle that is relatively enriched in incompatible trace elements (Albarède and van der Hilst, 1999; Kellogg et al., 1999; van der Hilst and Kárason, 1999). This is a particular case among the range of models that was being discussed (e.g., Davies, 1990b; Davies and Richards, 1992; Christensen and Hofmann, 1994). A major attraction is that it provides a convenient place to store trace elements for relatively long periods. There is circumstantial geophysical evidence in the form of a change in the character of seismic heterogeneity in this depth range (van der Hilst and Kárason, 1999), but the case is not very compelling and other explanations may suffice, as will be argued later in this article.

There is, however, a serious problem with this otherwise attractive model. It is that something like 50 to 70% of the Earth's internal radioactive heat sources would have to be located in this layer, to satisfy mass balance and thermal budget requirements. This heat, conducting across the upper interface of the layer, would generate a strong thermal boundary layer and rising thermal plumes that would be required to carry at least 50% of the Earth's heat budget. However, there is no evidence of such strong plumes at the Earth's surface. The discernible hotspot swells correspond with a total heat flow carried by plumes of only 6 to 10% of the Earth's heat budget (Davies, 1988; Sleep, 1990). Either the layer does not exist, or it has to be shown that the strong buoyancy flux coming off the top of it does not generate discernible topography or significant volcanism at the Earth's surface.

Thus, the reconciliation of the various kinds of evidence—geophysical, isotopic, and thermal—has remained a substantial puzzle. Although it has been mentioned only in passing so far, one study has seemed to go further than most toward resolving at least some of these issues. Christensen and Hofmann (1994) presented convection models featuring platelike surface motion and relatively viscous subducting "lithosphere." They simulated chemical heterogeneities by use of tracer points suspended in models of the convecting fluid. (In such models, the solid but deforming mantle material is treated as a viscous fluid, and often referred to as a fluid. This should not be confused with the true liquid produced by melting.) These models showed that if the tracers of oceanic crust are assigned an appropriately higher density than average mantle, then they tend to segregate to the bottom of the model, where they may remain for relatively long times. Although the mean residence time of segregated tracers was only ~1.4 Ga in their preferred model, conversion of tracer ages into lead isotopic evolution yielded apparent isotopic ages of ~2 Ga. This is because the tracers do not represent a single age from a closed source. In an open source, isotopic arrays tend to reflect older ages more strongly because of more rapid early decay.

The study by Christensen and Hofmann (1994) was a quantification of the original hypothesis of Hofmann and White

(1982), and it appears to support it quite strongly. The model does not generate a thick and continuous layer of segregated material like that hypothesized by Kellogg and others, and only ~14% of the nominally basaltic material is segregated. The segregated material occurs as separated "pools" below upwellings.

Christensen and Hofmann's (1994) work is instructive, and it gives a strong indication of the kind of model that might succeed. Nevertheless, there are important aspects of the models that might be improved upon or debated. Because of computational limitations at the time, the Rayleigh number is significantly below that for whole mantle convection, and there is uncertainty about how key results would extrapolate to full mantle conditions. The models were run for the equivalent of only 3.6 Ga, and no account was taken of the likelihood that the mantle was overturning faster in the past. Most of the models were heated 80% from below, which might exaggerate the stirring of the segregated layer by hot upwellings. One model was run with only 20% heating from below, and the fact that it yielded a similar degree of segregation to the other models raises doubt about whether the segregation really occurs mainly in the lower thermal boundary layer where subducted lithosphere is warmed and softened, as the authors suggested. Finally, even with only 20% bottom heating, the resulting erratic upwelling of buoyant sheets may significantly exaggerate the rate of stirring of tracers, as will be discussed further below.

Although Christensen and Hofmann's (1994) results give good agreement with observed isotopic data, only the age information in those data is really being strongly determined by the model. The spread of the isotopic ratios is not well determined, because it is dependent on choices of geochemical parameters that have significant uncertainty, as the authors acknowledge. This applies particularly to the U/Pb ratio. As well, the scatter in the isotopic plots is strongly dependent on the density of tracers used and on the scale of the sampling cells within which tracers are averaged.

The same effect must also apply in the mantle: the degree of isotopic scatter observed will depend on the spectrum of length scales of heterogeneities in the mantle source, the size of melting zones, and the degree of mixing during magma ascent. None of these factors is at all well known, and this means that isotopic scatter does not provide very direct information about the underlying processes generating and removing heterogeneities in the solid convecting mantle.

The models of Christensen and Hofmann (1994) are insightful and instructive, but substantial questions remain, and for the reasons just discussed, it seemed worthwhile to perform a new series of numerical experiments.

2. CONCEPTION OF THE MODELS

The particular choices made in setting up these numerical experiments were guided by some further considerations.

2.1. Convection

The stirring under consideration here is strongly affected by time dependence of the flow. In the mantle the two dominant sources of time dependence are probably the slow evolution of plate configurations and the ascent of new plumes. To account

for the former, Christensen and Hofmann (1994) included a subduction zone whose position oscillated. The rate of migration of the subduction zone was rather high compared with real subduction zones, which may have limited the formation of high viscosity regions. In the models below there are two subduction zones migrating more slowly, piecewise linearly, and at incommensurate periods. These aspects are closer to the character of observed plate tectonics, in which subduction zones migrate only slowly and the whole system lacks periodicity. Plumes seem to be secondary, both in volume and flow rate, so they may not add much effect to the that of the plate-scale flow, although ultimately this will need to be evaluated in three-dimensional models.

The viscosity depends on both temperature and depth. The depth dependence is a smoothed step increase through the mantle transition zone. Such a step, by a factor between ∼10 and 100, is indicated by modeling of positive geoid anomalies over subduction zones (Hager, 1984), and more recently by some models of postglacial rebound (Mitrovica, 1996; Lambeck and Johnston, 1998). In combination, these variations yield local regions of the lower mantle with viscosities several hundred times the upper mantle viscosity, and this evidently increases the residence time of the material considerably.

The models are run at the full whole-mantle Rayleigh number. In effect, this includes the full depth of the mantle relative to the thickness of the lithosphere. In combination with the viscosity variations just described, this allows buckling and folding of descending lithosphere to develop more fully than in the Christensen and Hofmann (1994) models. This may have some effect on the residence times of piles of cool, subducted fluid, and it has a clear relevance to the character of seismic tomographic images of the deep mantle.

The models are two-dimensional. This allows the models to have the full mantle Rayleigh number and a large number of tracers while still requiring a feasible computation time, which Christensen and Hofmann (1994) showed is necessary when the tracers carry anomalous density. It also permits more cleanly controlled experiments and more rapid exploration. Because the dominant plate-scale flow is approximately in the form of roll cells, two-dimensional sections may reasonably approximate important aspects of the flow. Certainly any conclusions will ultimately need to be tested with three-dimensional models, but there has been a recent tendency, now that three-dimensional calculations are more feasible, to overlook the continuing value and relevance of carefully posed two-dimensional models.

The models presented below are entirely heated from within for two reasons. The first is that less than 10% of the mantle's heat seems to enter from below: constraints from the Earth's surface topography indicate that plumes carry no more than 10% of the mantle heat budget (Davies, 1988; Sleep, 1990). If plumes come from the bottom of the mantle, as will be assumed here, then this is the rate at which heat flows from the core.

It is conceivable that stronger upwellings exist without producing discernible topography, but no persuasive case has yet been made, to my knowledge. Evidently it is often presumed that plumes might be dissipated within the mantle, but our current understanding of plume dynamics suggests that this is unlikely. One reason for this is that any heat that diffuses out of a plume merely heats adjacent material that then becomes entrained into the plume because it has also become buoyant. The heat carried by the plume therefore continues to ascend, as Griffiths and Campbell (1990) have demonstrated experimentally. It is possible in principle for lateral flow in the mantle to shear out a plume, but experiments indicate that the larger plumes, which carry most of the heat, will not be greatly deflected by the plate-scale flow in the mantle (Griffiths and Richards, 1989; Richards and Griffiths, 1989). It is therefore surprising that many recent models of mantle convection still have 50% or more of their heating entering from below and have clearly in evidence strongly buoyant upwellings that rise right to the surface. It is likely that these models would yield surface topography that deviates in obvious ways from what is observed, were their surface topography computed.

The second reason for heating the fluid entirely from within is that in two-dimensional models any upwelling is implicitly a sheet, rather than a thin column like a plume. The ascent of a sheet will necessarily disrupt cells driven by the upper thermal boundary layer. Such cell disruption seems to be an especially efficient way to remove heterogeneities (Davies, 1999a), and so the stirring rate would be artificially enhanced, possibly substantially. In three dimensional flow, on the other hand, hot fluid can ascend as a column, and the rising column of a plume will be much less disruptive of established plate-scale flow than a rising sheet. Therefore, it is a better approximation in these two-dimensional models to avoid the occurrence of upwelling sheets by reducing the bottom heating to zero. A proper evaluation of the effect of plumes on mantle stirring requires three-dimensional models. The hypothesis for the moment is that plumes do not have a major effect in three dimensions, but this will need to be tested in future.

2.2. Sampling the Mantle and Sampling Models

Some care is required regarding which characteristics of geochemical observations provide useful constraints on models of mantle convection, and regarding how the models are best compared with those observations. If isotopic scatter depends strongly on the scales of source heterogeneity, on the scale of melting, and on the magma ascent process, as suggested earlier, and if these aspects of the mantle are poorly known, then isotopic scatter may tell us more about the melting process than about the effect of mantle convection on heterogeneity. As well, one would have to be careful, when numerical models are used, to characterize the dependence of the predicted scatter on the density of tracers and the scale of sampling of those tracers.

Many summaries of mantle geochemistry have emphasized the relative uniformity of isotopes in midocean ridge basalts (MORBs), compared with the greater scatter of isotopes in ocean island basalts (OIBs, presumed here to be the products of plumes) (Jacobsen and Wasserburg, 1979; Allegre and Turcotte, 1985; Zindler and Hart, 1986). However, recent data are tending to reduce such perceived differences between MORBs and OIBs to within factors of 2 to 4 in both isotopic scatter and mean values, and also in trace element concentrations (Davies, 1999b; Honda and Patterson, 1999). Most of the features present in OIBs are also present in MORBs in more subdued form. The most notable exceptions to this are helium and argon isotopic ratios. The spread of helium isotopic ratios is ∼10 times larger in OIBs than in MORBs (Farley and Neroda,

1998), though the mean values are within a factor of 2. The perception of substantial difference is partly due to a focus on extreme isotopic values, which would be appropriate if the range reflects binary mixing of extreme sources, but not if it reflects a heterogeneous distribution of helium within the mantle. As well, there are peculiarities in the helium data that indicate an as-yet-unidentified process that selectively affects helium (Honda and Patterson, 1999). Argon also shows discordances with other isotopic data that suggest that the argon and potassium budgets of the silicate Earth are not fully understood (Albarède, 1998; Davies, 1999b).

The remaining robust difference between MORBs and OIBs is the greater trace element concentration and fractionation in OIBs, compared with a signature of source depletion in MORBs (Hofmann, 1997). Hofmann and White (1982), in their original proposal, emphasized this difference and proposed that it is due to a greater concentration of old oceanic crust in the OIB source than in the MORB source.

The relative depletion of MORBs and the apparent ages of MORBs and OIBs will be the characteristics most focused on in this study. These characteristics are reflected with perhaps the least complication in the isotopes of neodymium and lead, as already argued by Christensen and Hofmann (1994), although isotope diagrams are not calculated explicitly in this study. The degree of processing or degassing will also emerge as an important feature of the models.

We should bear in mind that when such characteristics are used, MORBs may not be providing us with information that is completely independent of the OIB ages. If MORBs exhibit a subdued form of most of the features evident in OIBs, notably in the refractory element isotopes, and lead isotopes in particular, then there is a question of how much of the MORB signature is due to contamination by OIB, whose higher trace element concentrations may tend to swamp the intrinsic signature of more depleted components.

Turning now to sampling of models, there has been a tendency to characterize the properties of tracers in convection models by sampling them through the volume of the fluid at a particular time, but this is not how we obtain samples of the mantle. MORBs evidently sample the top of the mantle in places where spreading centers happen to pull mantle material up. In this article, it is presumed that OIBs are produced by plumes rising from the bottom of the mantle, in which case they represent a sample of the very bottom of the mantle, from a region that may be only 10 or 20 km thick (Davies, 1990b; Davies, 1999a). Christensen and Hofmann (1994) sampled through the volume of their models for the sake of better statistics, but they recognized the approximation with the hope that interior tracers would not have changed too much before they reached a more realistic sampling region.

However, there is also an important conceptual implication of the way real OIBs are presumed to sample the mantle, namely that the distinctive signature of OIBs need not exist through a large volume of the mantle, but needs only to exist in the small region actually sampled. Thus, in particular, the OIB data do not require that the entire lower mantle, or a large fraction of it, be very different from the upper mantle. There are some mass balance requirements (Davies, 1999a), but these could be accommodated by a layer or region only a few hundred kilometers thick on average.

In the light of this discussion, tracers are sampled in the present study from the top and bottom of the models. The main characteristics sought are the age of last melting and variations in the concentration of tracers. Isotopic plots are not calculated explicitly, to keep uncertainties of geochemical parameters separate and to reveal the model dependence of the results more directly. The main effects turn out to be clear enough that more elaborate processing is not required in this initial report.

3. DESCRIPTION OF THE MODELS

3.1. Convection Models

The convection is computed in a 4×1 rectangular box, as depicted in Figure 1. The end walls are periodic. The base is free-slip and insulating. The top is divided into four segments, representing plates, and each has a prescribed surface temperature and horizontal velocity. The prescription of piecewise constant velocities permits better control of the locations of spreading centers and subduction and therefore yields a better-controlled experiment. The subducting plate velocities are equivalent to 5 cm/a and are actually about four times less than the velocities obtained in a comparable model with no plates and only depth-dependent viscosity.

A movie of the convection flow is included in an Electronic Supplement available on the journal's Web site. The features described here will be more clearly evident from the movie.

The central section of the surface, comprising the two inner plates, is intended to simulate the presence of continental lithosphere. The surface temperature of this section is set equal to the initial temperature of the interior fluid. In effect, this surface represents the hot base of continental lithosphere. Christensen (1996) first used this device, and it is important to obtain clean asymmetric subduction in models that cannot accommodate explicit internal faults. It was necessary to split this region into pieces that spread apart slowly in order that the "subducting" fluid from the outer plates detached cleanly from the surface most of the time, and particularly at times when the subduction zone retreats. This artifice has only a minor influence on the interior flow, slightly amplifying the circulation that is driven anyway by the adjacent subducting sheets.

The viscosity of the fluid has a strong temperature dependence multiplied by a moderate depth dependence. The temperature dependence is of a thermally activated form (Karato and Wu, 1993), represented here as

$$\mu = \mu_r \exp\left[\frac{E^*}{R^*}\left(\frac{1}{T} - \frac{1}{T_r}\right)\right] \quad (1)$$

where E^* is the activation energy, R^* is the gas constant, T is temperature, μ is viscosity, and μ_r is the viscosity at a reference temperature T_r, taken to be 1300°C (McKenzie and Bickle, 1988). The viscosity is bounded above at the value $100\mu_r$ so as to keep the iterative algorithm stable and also to account for the fact that the nonlinearity of the rheology of cold lithosphere will limit its stiffness to moderate values.

The depth dependence of the viscosity consists of a simple step smoothed over the depth range 670 to 960 km. Although the mean depth of this step is slightly greater than the main seismic discontinuity at 660 km, this form ensures low viscosities throughout the upper mantle. The upper 200 km of the
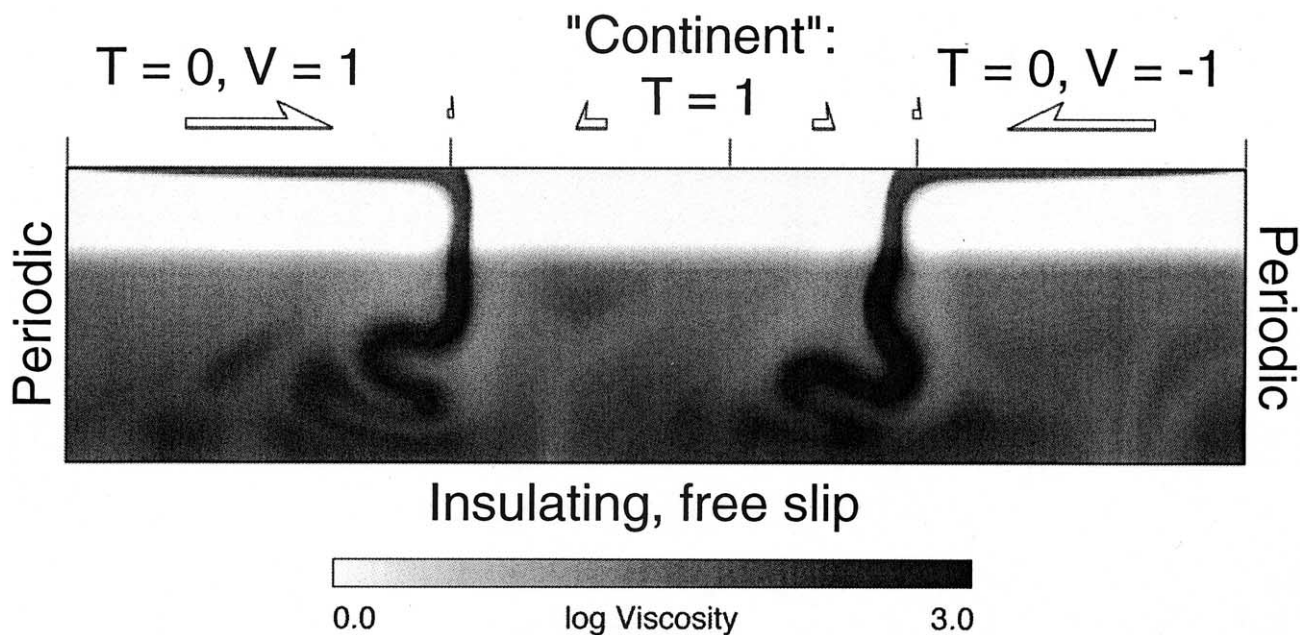
Fig. 1. Model setup and boundary conditions. The model simulates two "oceanic" plates on either side and a "continental" region in the middle, as described in the text. The interior shows the viscosity structure corresponding to Figures 3c,d A movie animation of the convection flow is included in the Electronic Supplement available on the journal Web site.

lower mantle through which the viscosity rises to its maximum value is still minor on the scale of the lower mantle thickness of more than 2200 km. Viscosity is the only spatially variable material property in these models.

The subduction zone "trenches" advance and retreat in a pattern that is prescribed by a sawtooth function. For the first one-sixth of a period, the trench advances with velocity $6a/\tau$, where a is the amplitude and τ is the period of the sawtooth oscillation. Between $\tau/6$ and $5\tau/6$ the trench retreats with velocity $-3a/\tau$, and in the final one-sixth it advances again with velocity $6a/\tau$.

In all of the runs reported here, the motion of the left-hand trench has dimensionless amplitude -0.5 and period $40t_t$, where t_t is the time to transit the depth of the box at the reference plate velocity. Thus, the "continental" plate effectively overrides this trench for an interval before retreating more slowly. The right-hand trench moves with a smaller amplitude of 0.3 and a period of $33t_t$, so it is also overridden by the adjacent "continent," which then retreats slowly. The mean positions of the trenches are at 1.5 and 3 (dimensionless), and the position of the break in the "continent" is at 2.25.

3.2. Tracers and Simulated Melting

The primary source of compositional heterogeneity in the mantle is the separation of a basaltic melt component from a depleted residue component at midocean ridges. The resulting oceanic crust/depleted mantle stratification is then returned into the mantle at subduction zones. The melting accomplishes the double task of sampling whatever net composition ascends into the melting zone and regenerating the heterogeneity to be reinjected into the mantle. These processes are simulated here by tracers.

Only one kind of tracer is used in these calculations. Christensen and Hofmann (1994) used two kinds of tracers, one representing basaltic melt composition and one representing the residue of melting. The two kinds were necessary because they included explicit calculations of the partitioning of trace elements between solid phases and melt in their models. However, in the present study, geochemical partitioning is not considered explicitly. In any case, most of the complement of highly incompatible trace elements is carried in the basaltic melt fraction, and a substantial fraction of moderately incompatible elements. This implies that much of the geochemistry can be implicitly accounted for simply by tracking a basaltic fraction, whether that fraction is explicitly separated as oceanic crust or combined into a homogenized pyrolite composition. Also, most of the mantle seems to have been previously melted and to be a heterogeneous mixture of depleted peridotite and eclogite, so associating the tracers with an explicit basaltic composition may in fact be a reasonably accurate representation of the mantle. Thus, it suffices for the present study to have only tracers representing the basaltic fraction.

The dynamic and thermal roles of melting and fractionation can also be accounted for the use of only basalt tracers. In some of the models below, the tracers are slightly denser than normal mantle, and it would also be possible to associate heat generation with the tracers. Regions that are depleted of tracers would then be implicitly buoyant or depleted in heat sources, respectively, relative to regions in which tracers become concentrated.

Melting zones in the models are defined under the notional oceanic plates by a maximum depth of decompression melting d_m. The melting zones do not extend under the central "continental" region because the upper boundary there is intended to

represent the base of thick continental lithosphere. Any tracer that is carried into a designated melting zone is placed in a notional oceanic crust above that point, by simply reducing its depth to 3.5 km. Because the oceanic crust is so thin on the scale of the mantle, it is not necessary to spread the oceanic crust tracers through a finite depth range. This procedure is otherwise quite analogous to that of Christensen and Hofmann (1994). The time of the tracer's "melting" is recorded, and the time of any previous melting is also preserved, so that the equivalent of the preeruption isotopic age is preserved.

The tracers are initially assigned uniformly in a grid pattern through the fluid. An initial dimensionless spacing of 0.00375 (equivalent to 11.25 km) yields 283556 tracers. Christensen and Hofmann (1994) used ~250000 tracers and found that this adequately eliminates artificial sedimentation of individual tracers. A further test is presented below that confirms the adequacy of this number of tracers in the present experiments.

3.3. MORB and OIB sampling

At the end of each run, the tracers present in the oceanic crust at the surface (i.e., presubduction) are treated as the equivalent of MORBs. A histogram of the ages of these tracers and their mean age are calculated.

A plume sampling zone is defined at the bottom of the model as a thin layer of thickness h_p, which is taken to be 20 km in all models presented here (Davies, 1990b). This choice is not critical because it affects mainly the statistics of the derived average age of material notionally sampled by plumes. The characteristics of the tracers that enter this zone are not changed, nor are they removed from the model. Because a relatively small volume of mantle material fluxes through the plume sampling zone, this is not expected to affect the results significantly. At the end of a run, the tracers within the plume sampling zone are considered to be the equivalent of OIB, and their age histogram and mean age are calculated.

3.4. Tracer Mass

For models that take account of a density difference, $\Delta\rho$, between the subducted oceanic crust and depleted mantle, it is necessary to specify how much basaltic component there is in the mantle, so that an appropriate mass anomaly can be assigned to each tracer. Because this basaltic component is implicitly assumed to be converted completely into oceanic crust when it is carried into a melting zone, the fraction of basaltic component is equivalent to the average melt fraction, f, within the melting zone. If there are N tracers and the computational box has volume V_B, then the volume of fluid per tracer is V_B/N. The volume of basaltic component per tracer is thus $f V_B/N$ and the mass anomaly per tracer is $m_b = f\Delta\rho V_B/N$. The mass anomaly carried by each tracer is assigned to the computational cell in which it resides at each time step of the computation. The value of f is determined by requiring the present oceanic crust thickness to be 7 km. For most models, the melting zone is assumed to be 70 km thick at present, so $f = 0.1$ (Table 2). Strictly speaking the value of f would decrease with time, but the uncertainties in how f would change are large (McKenzie and Bickle, 1988), and for the present exploratory calculations,

the effect is subsumed into the prescribed decrease of melting depth with time (Table 2).

Irifune and Ringwood (1993) estimated that oceanic crust would be 100 to 200 kg/m³ denser than average mantle within the upper mantle. It may be less dense through part of the transition zone. Kesson et al. (1994, Kesson et al., 1998) estimated that the density excess varies from +40 kg/m³ to −30 kg/m³ through the lower mantle. In other words, they suggest that oceanic crust becomes less dense than average mantle within the deepest mantle. If this estimate is confirmed, it would complicate the hypothesis explored here and by Christensen and Hofmann (1994), but because there are significant uncertainties in estimating relative densities at the bottom of the mantle, it will be assumed here that the oceanic crust remains a little denser than average mantle.

For the sake of this exploration, a constant density difference is assumed. The effects of values of 50 to 100 kg/m³ are illustrated in the results presented below. The ratio of this difference to the maximum thermal density anomaly is then 0.4 to 0.8. This is smaller than the ratio of 1.5 at the bottom of the models of Christensen and Hofmann (1994), who included a decrease of thermal expansion with depth by a factor of ~6 and a decrease of compositional density anomaly by a factor of ~2.

3.5. Earth Time and Model Time

If the mantle was hotter in the past, as is widely believed, then its viscosity would have been lower and it would have been overturning faster. This means that heterogeneities would have been stirred to a greater extent in the early part of Earth history. As well, the depth of decompression melting would have been greater. This expectation combines with the faster overturn to imply that mantle material would have been processed through melting zones much more rapidly early in the Earth's history. The faster overturn is approximately accounted for in this study by running the models for an equivalent number of overturns, but at a steady rate, and by then converting model time into an equivalent Earth time in the calculation of tracer ages. The deeper melting is accounted for by making the melting depth a function of equivalent Earth time.

Plate velocity is proportional to the square of surface heat flux, and in thermal evolution calculations, the surface heat flux of the mantle approximately tracks the decline in radioactive heat generation (Davies, 1999a). Therefore, it is assumed here that plate velocity declines as the square of the declining heat generation. The decline of heat generation is, to a sufficient approximation for this study, taken to be a simple exponential with a decay constant $\lambda = 0.26 \text{ Ga}^{-1}$. This assumption implies that the heat generation 4.5 Ga ago was 3.22 times its present value, and plate velocities would have been 10.4 times faster. The model time, t_m, equivalent to a particular Earth time, t_e, is assumed to be the time taken for a plate to travel the same distance as in the slowing Earth. This is calculated as follows.

Counting Earth time, t_e, to be zero at the beginning of Earth history, the heat production, H, is $H = H_0\exp[\lambda(a_E - t_e)]$, where H_0 is the present heat production and a_E is the age of the Earth, taken here to be 4.5 Ga. The plate velocity is then $v = v_0\exp[2\lambda(a_E - t_e)]$, where v_0 is the present velocity. The distance traveled in this time is the integral of v:
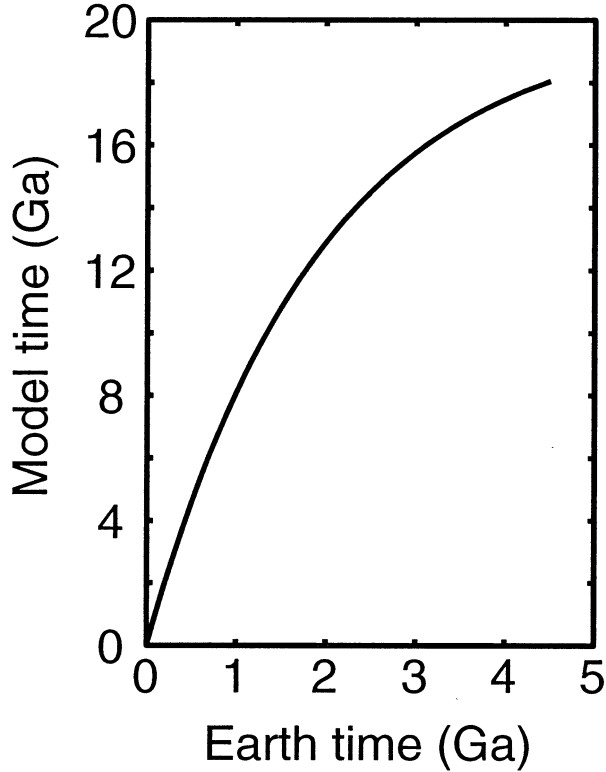
Fig. 2. Relationship between model time and Earth time (Eqn. 3). The models are run at constant Rayleigh number corresponding to present mantle conditions and rate of overturn; however, the mantle was hotter and overturned more rapidly in the past. Thus, ~18 Ga of steady model time is required to match 4.5 Ga of slowing Earth overturns.

$$s = \frac{v_0}{2\lambda} e^{2\lambda a_E} (1 - e^{-2\lambda t_e}) \qquad (2)$$

To travel the same distance at a constant speed equal to the present average plate speed, v_0, requires model time $t_m = s/v_0$. By substituting Eqn. 2 into this relationship and rearranging, the scaling from model time to Earth time is found to be

$$t_e = -\frac{1}{2\lambda} \ln \left[1 - 2\lambda t_m \exp(-2\lambda a_E) \right] \qquad (3)$$

With the values given above, 18.04 Ga of model time is required to achieve the stirring equivalent to 4.5 Ga of Earth time. Fig. 2 shows the relationship between the two timescales.

The decrease in the melting depth is assumed for simplicity to be linear with Earth time, given its substantial uncertainty, and it is specified by an initial value and a final value. This procedure of scaling the model time and melting depth implies that plate tectonics, or something equivalent, has operated throughout Earth history. There are good reasons why this might not be so (Davies, 1992), but further discussion of this point will be deferred until after the results are presented.

3.6. Computations

Incompressible Stokes flow is assumed. The equations are given, for example, by Davies (1999a). Finite difference ap-

Table 1. Convection parameters.

Depth of layer (D)	3000 km
Reference viscosity (upper mantle, μ_{ref})	3×10^{20} Pa.s
Viscosity step factor	30
Depth of viscosity step	0.29
Thickness of viscosity step	0.0625
Thermal activation parameter (E^*/R^*T_{ref})	20
Reference temperature (T_{ref})	1573°K
Activation energy (E^*)	260 kJ/mol
Reference heat flux (q_{ref})	35.5 mW/m^2
Reference plate velocity (V_{ref})	50 mm/a
Thermal expansion (α)	2×10^{-5} °C^{-1}
Thermal diffusivity (κ)	10^{-6} m^2/s
Specific heat (C_P)	750 J/kg°C
Reference density (ρ)	4000 kg/m^3
Conductivity ($K = \kappa\rho C_P$)	3 W /m°C
Gravitational acceleration (g)	10 m/s^2
Rayleigh number, $R_q = g\rho\alpha D^4 q_{ref}/K\kappa\mu_{ref}$	2.5×10^9
Peclet number, Pe $= V_{ref}D/\kappa$	4750

proximations are used on a uniform 128 × 512 grid. The adequacy of this resolution was tested by comparing with the results of using a coarser grid (64 × 256). Some details of the flow were different on the coarser grid, but the aggregate results reported here were not changed significantly.

The flow equations are solved by a multigrid method, and the heat equation by an alternating-direction implicit method with weighted upwind differencing (Davies, 1995). The code has been benchmarked against published examples (Blankenbach et al., 1989). General input parameters are given in Table 1. Tracers are advected by a fourth-order Runge-Kutta method, which previous experience has shown to be adequate and which Christensen and Hofmann (1994) found to close a steady streamline with an accuracy of 10^{-6}.

Perhaps it is worth noting that both the tracer stirring and the flow itself seem to be chaotic in these experiments. The tracer stirring is chaotic because tracers that closely approach a stagnation point of the flow may be deflected onto quite different paths by minor influences on the flow. Thus, in the long term, tracer paths tend to diverge roughly exponentially (because the distance between them tends to be progressively doubled). The buckling of descending lithosphere that will be seen in the results is an exponentially growing instability that can cause the fluid buoyancy also to be advected chaotically. Thus, these experiments will not be reproducible in detail, except with the identical code running on an identical computer. Only aggregate properties are significant.

4. RESULTS

The series of models presented here illustrates the dependence of model behavior on a number of factors. The question of which factors might be most relevant to the mantle is taken up in the discussion.

4.1. Passive Tracers

Figure 3 shows a selection of frames from a run with passive tracers, in other words tracers with no associated density anomaly. A movie animation of selected segments of this run is
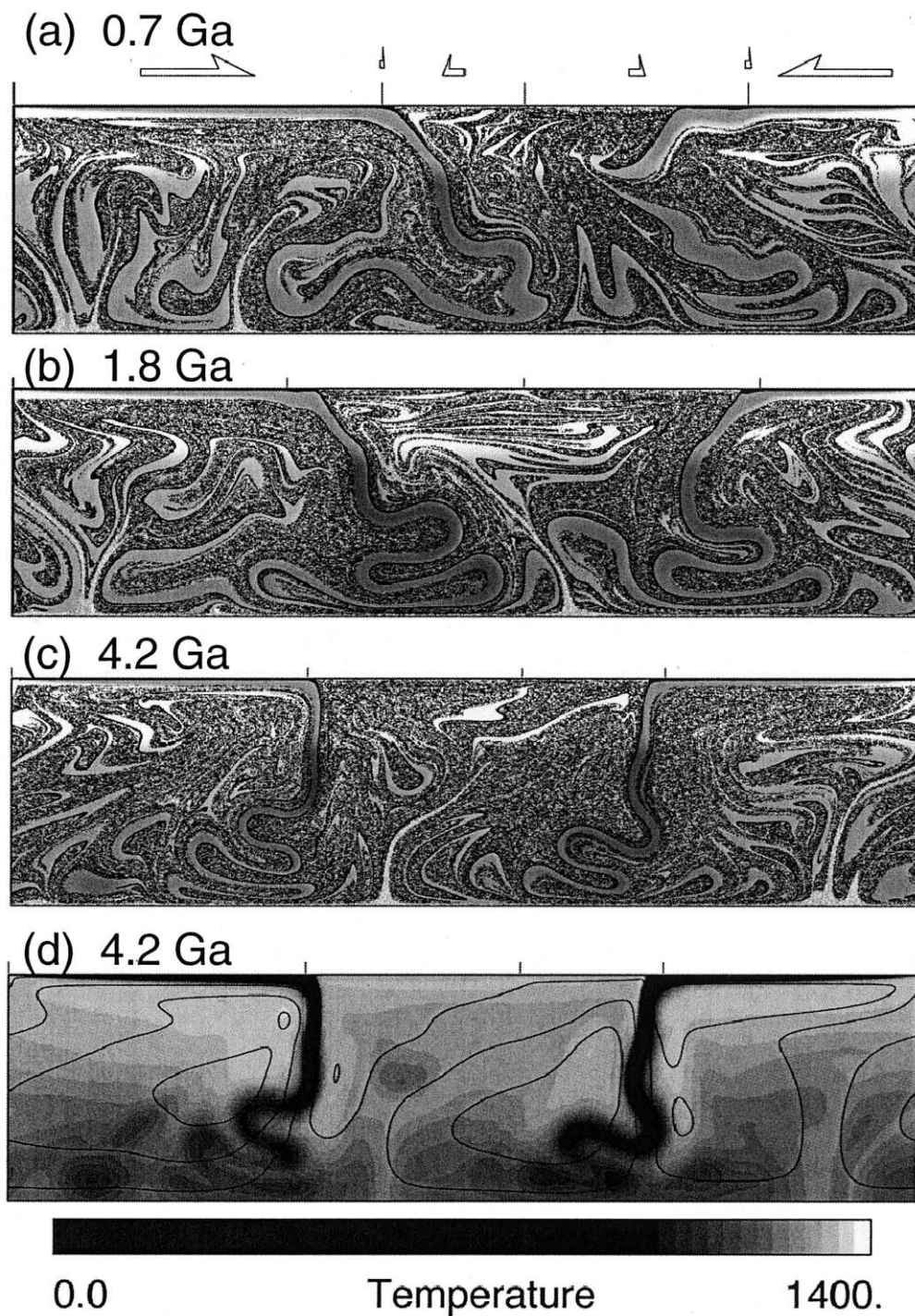
G. F. Davies

Fig. 3. Frames from the model Passive (Table 2), with passive tracers, labeled with Earth time. (a–c) The tracers are plotted against a muted grayscale of the viscosity structure (compare Fig. 1). Tracers that rise into the "melting" zone under the oceanic plates are placed into the thin crust, leaving a depleted zone beneath. This differentiated structure is then subducted and stirred by the convective flow. (d) Temperature at 4.2 Ga plotted in grayscale, with streamlines superimposed. Streamlines show the instantaneous direction of fluid flow. A movie animation of this model is included in the Electronic Supplement.

included in the Electronic Supplement. Parameters specifying this and following models are given in Table 2. The melting depth decreases from an initial value of 140 km to 70 km in this model, and this accounts for the thinning of the empty "deplet-

ed" ribbons through the sequence. There is a striking persistence of quite thick depleted regions in the earlier stages of the model.

The contortions, and much of the stirring, in this model are

Table 2. Specifications of the models and remaining primitive fractions.

Variable	Fig. 3 (Passive model)	Fig. 6 (Dense 100 model)	Fig. 8 (Deepmelt model)
Tracer density (kg/m³)	0	100	50
Melting depth (km)			
Start	150	150	240
End	70	70	100
Basaltic (melt) fraction	0.1	0.1	0.07
Primitive remnant (%)	2.5	1.9	0.3

enhanced by the buckling of subducting "lithosphere" as it sinks into the high-viscosity deep mantle (the viscosity structure corresponding to Figs. 3c, d is shown in Fig. 1). Later examples will show that there are times when subduction is oblique, with less buckling, as a result of episodes of substantial horizontal shearing between the top surface and the lower mantle. The stirring is further promoted by the time dependence resulting from the imposed migration of the subduction zones. With time, subducted material becomes stirred down to progressively finer scales, the finest scale that can be discerned being limited by the number of tracers in the model.

The detachment of subducted material from the top surface is asymmetric and fairly clean most of the time, in this and all of the other models. Thus, the models seem to give quite a good simulation of real subduction. An exception is evident at the right-hand subduction zone in the top frame, where the right-hand plate is being overridden by the continent, and the plate material has not immediately subsided. This is analogous to an existing situation under Chile and an inferred situation under western North America in the early Tertiary.

Some characteristics of the tracers after 4.17 Ga of Earth time are summarized in Figure 4. Figure 4a shows the distributions of the ages of notional MORB and OIB. A striking result is that the mean ages of both MORB (2.7 Ga) and OIB (2.57 Ga) are well in excess of apparent lead isotopic ages from the mantle of ~1.8 Ga. As will become clearer, this result seems to be due to the combination of the long run time, the reasonable simulation of surface plates and the high viscosity of subducted lithosphere locally in the lower mantle. Viscosities of several hundred times the viscosity of the upper mantle persist through quite large volumes of the lower mantle (Fig. 1).

Models without plates and stiff slabs yield much shorter mean ages. An analogous model in which the temperature dependence of the viscosity and the surface plate velocities were eliminated yielded a mean MORB age of 600 Ma and a mean OIB age of 300 Ma after a comparable amount of stirring. This was in part because the flow velocities were several times higher in the upper mantle and many times higher in the lower mantle. A comparable model by Christensen and Hofmann (1994), with only depth-dependent viscosity, yielded a mean age in the "pools" at the bottom of the model of only 360 Ma.

Christensen and Hofmann (1994) did not report a mean age for their case with passive tracers. However, the case with the lowest assumed tracer density contrast yielded a mean age of 870 Ma, and the passive tracer case would have yielded a

substantially smaller age again. Only by including tracers with a substantial density excess did Christensen and Hofmann (1994) obtain ages much greater than 1 Ga. The main reason for their smaller ages compared with Figure 3 would seem to be the much shorter run time of their models: 3.6 Ga with no allowance for faster overturn in the past. This is only 20% of the 18-Ga model time of the present runs.

Another important result is that 97.5% of the tracers have been processed through a melting zone (Table 2). In other words, only 2.5% of the fluid is primitive, in the sense that it has not been processed through a melting zone. This accords with the lack of compelling evidence for any primitive signature in refractory element isotopes from mantle-derived rocks (Hofmann, 1997). In fact, because of the deeper melting zone at earlier stages, more than 80% of the fluid is processed within the first billion years of Earth time (Fig. 5), which corresponds with about ~45% of the model time (Fig. 2).
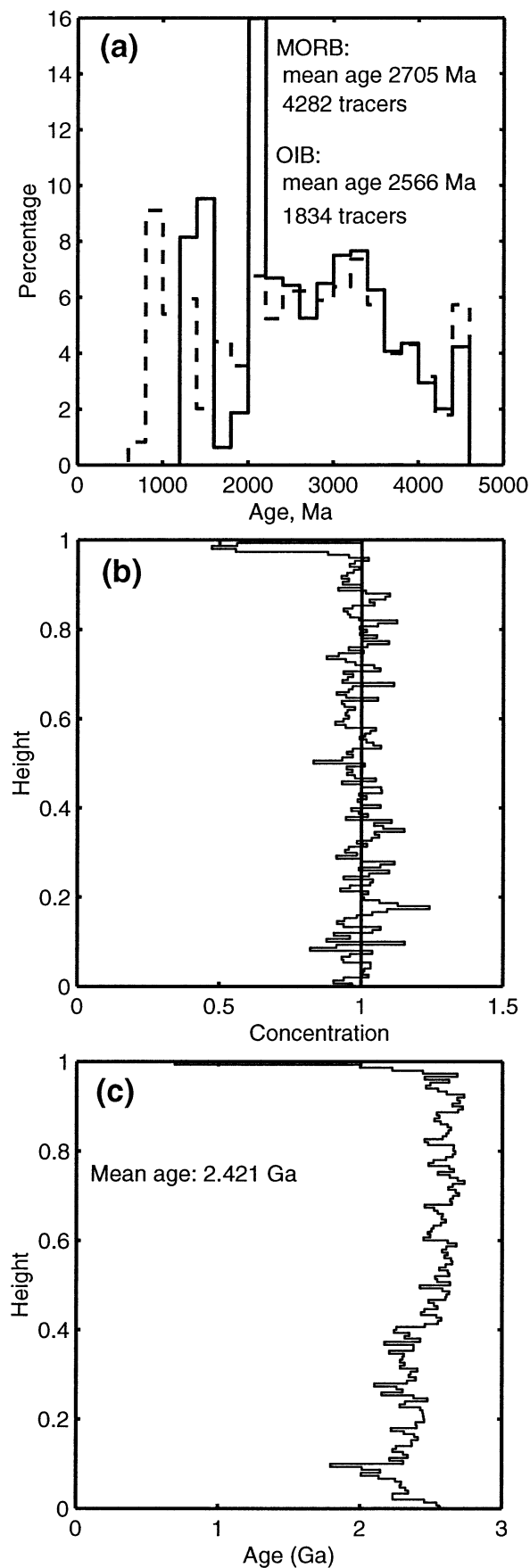
To provide a reference for later models in which tracers are not neutrally buoyant, Figure 4b shows the horizontally averaged concentration of tracers as a function of depth. The averages are taken within layers only 20 km thick, so as to reveal any fine structure. This thickness also corresponds with the thickness of the plume sampling zone at the base. There is considerable small-scale spatial fluctuation, reflecting the heterogeneity evident in Fig. 3, but no other significant vertical structure. The minimum near the top reflects the depletion of the fluid as it rises into the melting zone.

Figure 4c shows the mean age vs. depth, averaged in 20-km-thick layers. This allows us to see the relationship of ages in the interior to the OIB age of 2.57 Ga, which corresponds to the lowest layer. There is spatial fluctuation both on the fine scale and on larger vertical scales, implying that the OIB age would fluctuate in time by as much as several hundred million years, as is indeed evident in earlier samplings (data not shown). The MORB age also fluctuates with time, but tends to be more stable, usually varying by no more than ~100 Ma.

The relatively smaller fluctuation of MORB ages compared with OIB ages is in qualitative agreement with the smaller scatter of isotopic ratios discussed earlier, but great significance should not be attached to this result at this stage. Figure 3 gives a qualitative impression that the upper mantle of the models has less large-scale heterogeneity than the lower mantle, but this has not been quantified. As well, the fluctuations depend on the size of the sampling volume, which is greater for MORB than for OIB in these models, but we do not have a clear idea of what the sampling volumes are in the real mantle, as was discussed earlier.

The age tends to decrease toward the lower part of Figure 4c. This is a persistent feature of passive-tracer models. The decrease presumably reflects the fact that it takes less time for fluid to reach the bottom than for it to complete the round trip to the bottom and back up. This feature is evident also in the histograms of Figure 4a, where the youngest OIB ages are about half of the youngest MORB ages. This implies as well that not much of the fluid recirculates just in the upper part of the model, as is also confirmed by the streamlines in Figure 3d.

The ages that have emerged from this model are of course considerably greater than the apparent lead-isotopic ages observed in MORBs and OIBs (Hofmann, 1997). This overestimate is especially marked if the isotopic arrays tend to reflect

Fig. 4. Tracer characteristics from the model Passive (Fig. 3). (a) Age histograms of the MORB (solid lines) sample and the OIB (dashed lines) sample at the end of the run. (b) Horizontal averages of tracer concentration. The tracer concentration shows small-scale heterogeneity, but neither plot shows any other significant vertical structure, apart from the depleted melting zone near the top. (c) Horizontal averages of the age of tracers (i.e., time since last "melting").
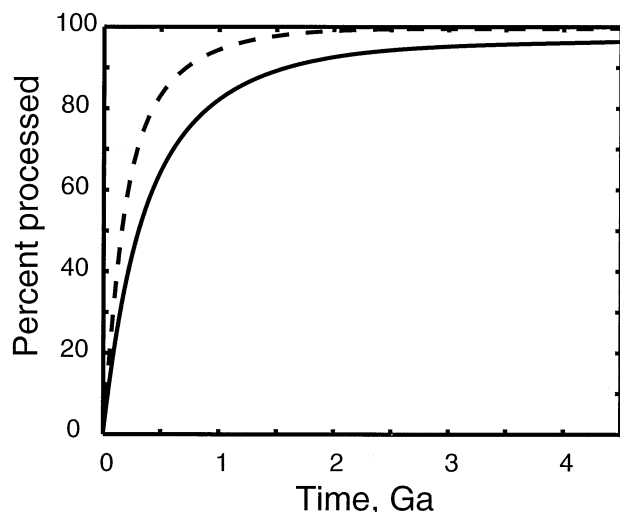
older tracers more strongly, as Christensen and Hofmann (1994) showed to be the case in their models. However, there are several reasons why the present model might have overestimated the ages, as will be discussed after other model results have been presented.

4.2. Heavy Tracers

Figure 6 shows the distributions of tracers and temperature from the model Dense100, in which the tracers are assumed to carry a mass corresponding to an excess density of 100 kg/m^3. The subduction of the right-hand plate is episodic at this time, as in Figure 3a.

In the lower left of Figure 6a is a large pool of heavy tracers that, because of the periodic boundary conditions, is continued in the lower right of the model. To reveal this pool by using only the gray tones of this figure, tracers that have passed through the plume sampling zone at the bottom are plotted as white dots. The pool is revealed as having a white outline with a mottled interior, the mottling being the result of the entrainment of tracers that have not passed through the plume sampling zone. Two smaller columns of white tracers can also be seen. These pools are quite analogous to those reported by Christensen and Hofmann (1994).

There are other significant features in Figure 6a. In the upper left, several concentrations of tracers have formed. These concentrations have a higher mean density than surrounding fluid, which has caused them to form sinking diapirs in the upper mantle. In the deeper fluid on the left, in contrast, are four regions of fluid that are devoid of tracers and therefore relatively buoyant. These regions were formed originally as a result of buckling of subducted "lithosphere." Their buoyancy is causing them to rise buoyantly in Figure 6. Smaller-scale rising diapirs of tracer-depleted fluid can also be seen in the upper right of the model, and less distinctly under the left hand plate.

Several profiles of the horizontally averaged tracer concentration from this model are shown in Figure 7 (the differences between the profiles are explained in the next section). There is a large increase in tracer concentration near the bottom. This corresponds to the large pool of tracers just noted. However, a second important feature is also revealed, namely that there is a gradient of tracer concentration through the upper mantle. This indicates that the small-scale diapirism noted above has resulted in a significant separation of tracer concentrations from tracer-depleted fluid within the upper mantle. This phenomenon has not been reported before. Its potential significance will be discussed below.

The mean OIB age from this model is 3.38 Ga, considerably greater than the mean MORB age of 2.64 Ga (Table 3). The large OIB age indicates that the tracers in the bottom pool tend to be trapped there for a long time, as has been reported by

Fig. 5. Cumulative processing of tracers vs. Earth time for the models Passive (Fig. 3; solid) and Deepmelt (Fig. 8; dashed).

4.3. Numerical Resolution and Tracer Resolution

The small-scale features evident in the upper mantle of Figure 6a correspond to scales of 100 km or more in the real mantle. These are still resolvable by the computational grid, which has a spacing corresponding to ~25 km. The formation of small-scale diapirs in the upper mantle of the model in Fig. 6 has not been observed in previous studies. To check that there is a sufficient concentration of tracers to resolve this process properly, the model with heavy tracers was run twice, first with the standard number of tracers and then with 3.5 times as many tracers (997501 tracers, with an initial spacing of 0.002, equivalent to 6 km), which in effect provides finer resolution of the effects of heavy tracers. Figure 6 is from the model with the higher number of tracers.

Profiles of tracer concentration from these models are compared in Figure 7. The black profiles are from the model with the standard number of tracers at Earth times 3.5 Ga (thin) and 4.55 Ga (thick). The gray profiles are from the model with the higher number of tracers (and thus finer resolution) at Earth times 3.4 Ga (thin) and 4.4 Ga (thick). Both the upper mantle gradient and the bottom concentration are robust, with regard both to time and to the tracer resolution. The coarse tracer resolution (black) may slightly overestimate the upper mantle gradient, but this test indicates that it is a real feature of the physics. On the other hand the coarse tracer resolution may underestimate the concentration near the base of the model, but the difference is not enough to conclude that this feature is an
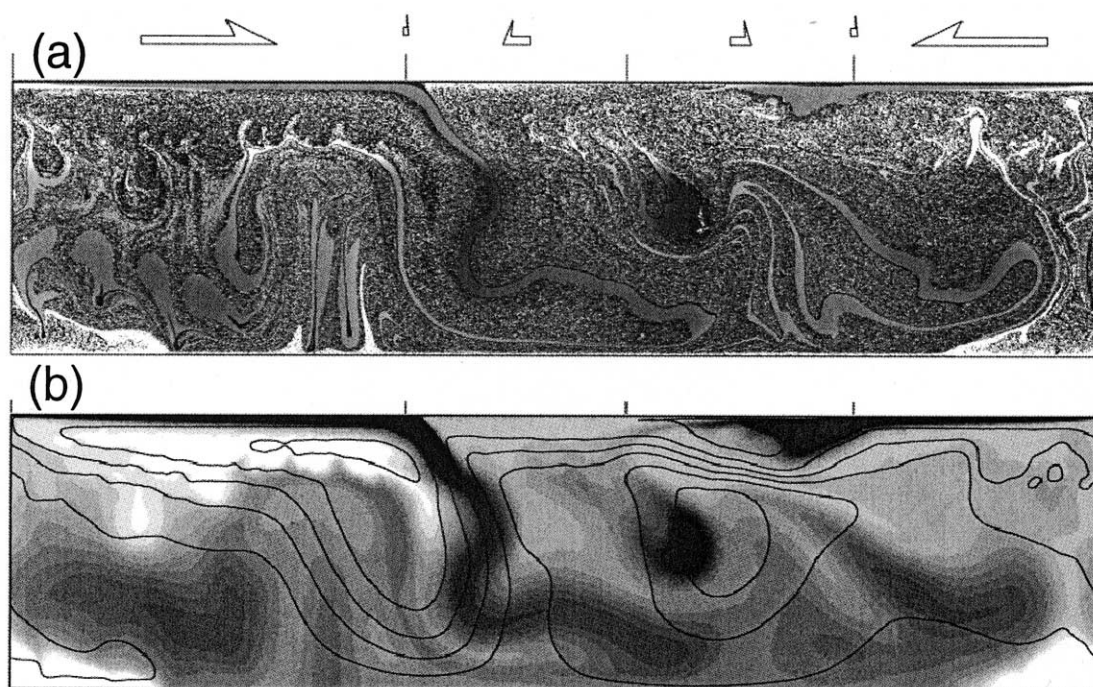
Christensen and Hofmann (1994). This is confirmed by age histograms (data not shown), which show that the OIB age distribution is strongly skewed to older ages. This model yields OIB ages that are too extreme to correspond with the mantle, but it serves to reveal important effects of heavy tracers.

Fig. 6. Late frames (at Earth time 4.36 Ga) from the model Dense100, which has 997501 tracers with an associated density of 100 kg/m³. (a) Tracers. In the upper mantle, there are sinking diapirs of concentrated tracers and rising diapirs of tracer-depleted fluid. At the base is a large pool of dense tracers, outlined by the white tracers that have passed through the plume sampling zone. (b) Temperature. Tracer concentrations tend to be associated with warmer fluid because the tracers inhibit circulation of associated fluid.
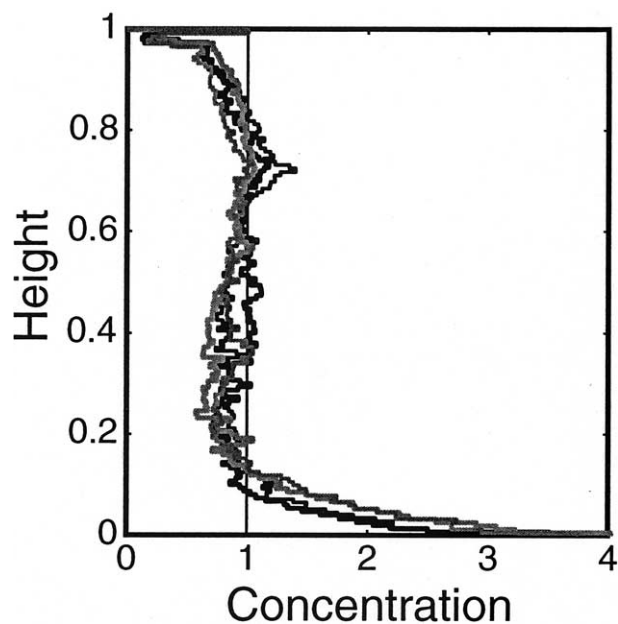
Fig. 7. Tracer concentration profiles from the model Dense100 (Fig. 6). This Figure also serves as a test of the effect of absolute tracer concentration by comparing models with the standard 283556 tracers (initial spacing 0.00375; black profiles) and 997501 tracers (initial spacing 0.002; gray profiles; model Dense100). The profiles show tracer concentration, relative to the model average, at two late times for each model: 3.5 Ga (thin) and 4.55 Ga (thick) for the standard model, and 3.4 Ga (thin) and 4.4 Ga (thick) for model Dense100.

artifact. Thus, for the present exploratory study, the coarse tracer resolution is adequate.

4.4. Deeper Melting Zone

The effective depth of the zone from which melting scavenges the elements of relevance to this study is not very well determined, so it is useful to see the effect of varying the depth of the melting zone. This is especially pertinent because the effectiveness with which an element is scavenged will depend on its incompatibility: more incompatible elements will tend to be scavenged by the first small degrees of melting, and hence effectively from a greater depth than less incompatible elements. A thicker melting (and scavenging) zone will tend to process mantle material more rapidly. A thicker melting zone also affects the *buoyancies* of depleted zones, buoyancy being proportional to the *mass* anomaly (density anomaly times volume), not just to density anomaly.

Results from a model in which the melting depth varies from

Table 3. Mean ages of tracers.

Figure	Model	Mean ages (Ga)			Mean ages (<2.7 Ga)	
		MORB	OIB	Model	MORB	OIB
3	Passive	2.71	2.57	2.42	1.98	1.71
6	Dense100	2.64	3.38	2.52	1.93	1.72
8	Deepmelt	2.23	2.62	2.05	1.79	1.37

240 km initially to 100 km at the end, and with tracers having a density anomaly of 50 kg/m^3, are shown in Figures 8 and 9. A movie animation is included in the Electronic Supplement. Figure 8a shows the tracer distribution at the relatively early stage of 1.5 Ga (Earth time), when the melting zone is still ~180 km thick. It is remarkable how large are the regions devoid of tracers in the lower mantle. The larger volumes of depleted fluid enhance the segregation of tracers, in spite of the lower density difference in this model, and a significant pool of heavy tracers is evident in the lower left of the model. Much segregation at a smaller scale is also evident in the upper mantle. In fact there is a clear suggestion in this image that large-volume rising diapirs break into smaller diapirs as they enter the lower-viscosity upper mantle. At the later Earth time of 4.4 Ga (Fig. 8b) each of these features is still evident, although they are less dramatic because of the thinner melting zone and consequent smaller-volume depleted zones.

These features are also reflected in the vertical profiles of Figure 9, where there is a strong gradient of tracer concentration through the upper mantle and another concentration at the base. The average age within the bottom concentration is distinctly greater, indicating that tracers are trapped there for long periods (Fig. 9c). This greater age is reflected also in the age histogram of the OIB sample (Fig. 9a), which is quite bimodal because of a substantial number of tracers older than 3.5 Ga.

The mean MORB age of 2.23 Ga (Fig. 9a, Table 3) is younger than in the previous models, reflecting the more rapid processing in this model. The mean OIB age of 2.62 Ga is distinctly greater than the MORB age because of the segregation at the bottom of the model.

By the end of this run, 99.7% of the fluid has been processed (Table 2). The cumulative percentage processed in this model is included in Figure 5 (dashed curve): more than 80% is processed within the first 500 Ma.

5. IMPLICATIONS

The models presented here are exploratory, and not intended to be definitive simulations of the mantle. They demonstrate at least one new phenomenon (upper mantle segregation) and some quantitative results significantly different from those of previous studies. That the results are reasonably reliable (in the sense that the physics of the problem have been appropriately included in the models) is suggested by the comparisons with previous work that have been discussed (or are discussed below), which indicate plausible reasons for the differences between the different studies. Further work will be required to substantiate this claim more fully.

There are other sources of uncertainty or difference. One is the intrinsic unsteadiness of the models that, for example, causes the age estimates to fluctuate with time. This is elaborated below. Another source of difference is that different model parameter values may reasonably be chosen. Some indications of the sensitivity of results to some key parameters will be noted in the following discussion. However, the purpose of this article is not to fully explore this potentially large topic but merely to show some results that are plausible. The latter demonstration suffices to show that this kind of model may deserve more attention than it has received to date.
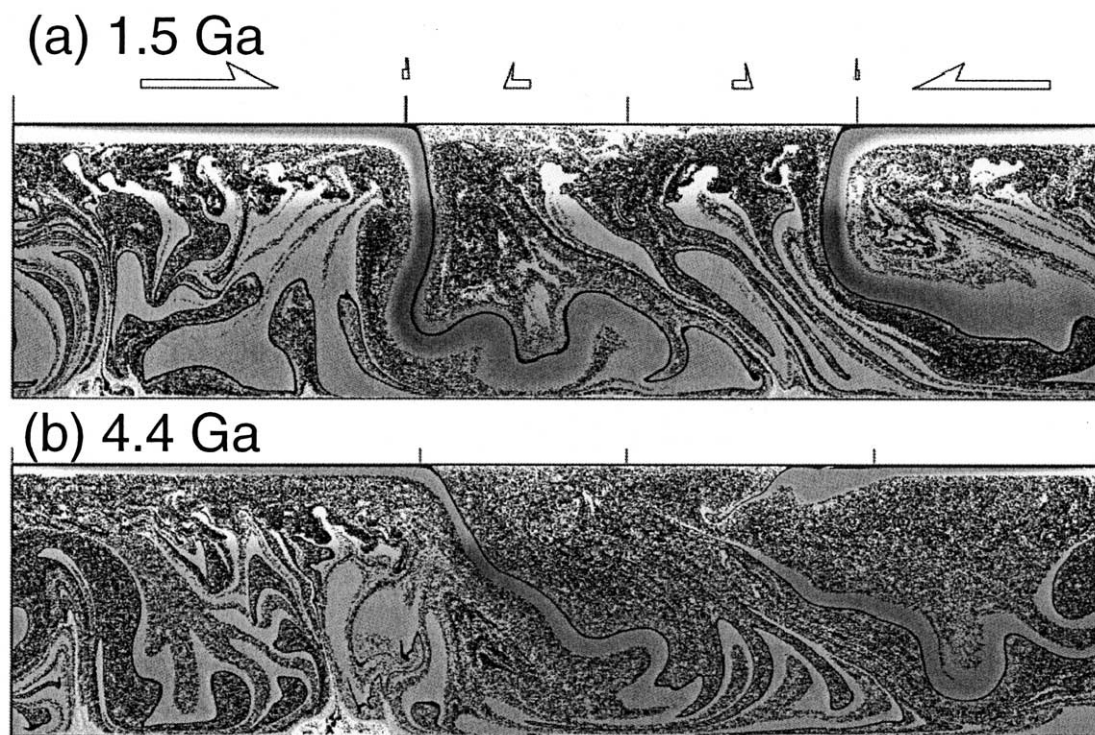
Fig. 8. Frames from model Deepmelt, in which the melting zone depth varies from 240 to 100 km and tracers have an excess density of 50 kg/m^3. Note the large tracer-depleted zones and the obvious rising and sinking diapirs in the upper mantle at the earlier time. Although the tracers have only half the density anomaly as in Fig. 6, the thicker depleted zones still yield significant segregation of tracers. A movie animation of this model is included in the Electronic Supplement.

5.1. Tracer Ages

The most significant result from these models is perhaps the age information, because it removes the perceived obstacle that this kind of model cannot account for the nearly 2 Ga apparent age of isotopic heterogeneities in the mantle and thus extends the range of potentially viable models. With a set of assumptions and parameter values well within the range indicated by independent constraints, the models have yielded ages between 2.2 Ga and 2.7 Ga, more than enough to account for the observations.

The comparisons among the models, and with related models that have already been discussed, suggest that the main reasons for the ages being greater than in previous studies are, first, the inclusion of a reasonable representation of the lithosphere, especially the platelike behavior at the surface and the higher viscosity of subducted material; second, the vertical viscosity structure; and third, simply to run the models for long enough, taking account of faster overturn of the mantle in the past.

There are several reasons why these models might have overestimated the ages of mantle heterogeneities.

(1) The viscosity of the subducted material in the lower mantle might be too high in the models. As noted earlier, models with no temperature dependence yield residence times of only a few hundred million years. Thus, a modest reduction in slab viscosity would presumably reduce the residence time of material in these regions.

(2) The models involve the implicit assumption that plate tectonics, or something like it, has been running since early in Earth history. A different possibility is that only the subcrustal part of the cool thermal boundary layer subsided into the lithosphere, leaving relatively buoyant mafic crust at the surface (Campbell and Griffiths, 1992; Davies, 1992; Campbell, 1998). If basaltic material was not subducted in significant volume until, say, 2.7 Ga ago, then the older parts of the age histograms would not be present and the mean age would be younger.

(3) The upper thermal boundary layer must have been doing *something* to remove heat from the mantle during the Archean, otherwise the interior would have been heating instead of cooling (Davies, 1992, Davies, 1999a). Another possibility is that the formation of sialic continental crust in the Archean was accompanied by the formation of a dense and depleted residue that sank into the mantle (Zegers and van Keken, 2001). Such material would thereafter be relatively invisible geochemically because it would be refractory and therefore would produce little magma, and because its depletion would mean that even if it did melt it would contribute little to the trace-element signatures of magmas reaching the Earth's surface. Thus, in this case also, the older parts of the age histograms would be missing and the mean ages would be younger.

(4) In spherical geometry, the volume of the lower mantle relative to the upper mantle is reduced, and the local flux of heat from the core is increased by a factor of 3.3, so plumes will be relatively more significant at the bottom of the mantle. The purely geometric factor is probably not very important because
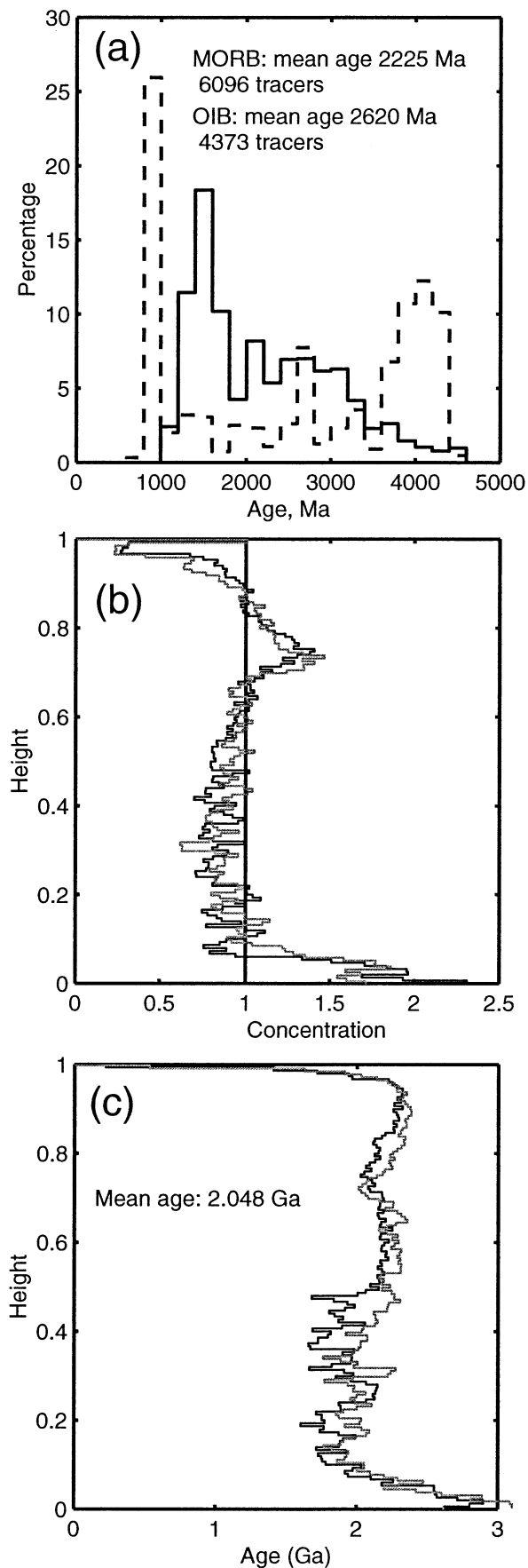
the lower mantle comprises about two-thirds of the mass of the mantle, and in the present incompressible models 71% of the fluid is below the middle of the viscosity step. The effect of stronger plumes might be significant, but comparison of the models of van Keken and Ballantine (1998), which have 60% bottom heating, with those of Hunt and Kellogg (2001), which have no bottom heating, suggests that this is not a very important factor.

These possibilities can be investigated in future, but the potential of points 2 and 3 can be easily estimated simply by eliminating tracers older than (say) 2.7 Ga from the calculation of mean ages. The resulting mean ages are included in Table 3. They fall mostly between 1.7 and 2 Ga, which suggests a satisfactory agreement with observations, although the tendency of lead isotopic arrays to emphasize the older tracers, as demonstrated by Christensen and Hofmann (1994), might still leave some discrepancy.

The main significance of these models at this stage is not that they tell us exactly how to account for the observed apparent ages, but that they clearly demonstrate the potential to do so, whereas that potential has not been obvious to date. In fact key observations are accounted for so readily that there is room for significant variation of the models, and trade-offs of model parameters while retaining consistency with observational constraints.

5.2. Rates of Processing

The combination of faster overturning of the mantle and a thicker melting zone in the past results in most of the fluid being processed through the melting zone. The percentage of unprocessed tracers ranges from 2.5% for the case of the thinner melting zone down to 0.3% for the thicker melting zone. The degree of processing is dramatically higher than, for example, the models of van Keken and Ballantine (1998, van Keken and Ballantine 1999), in which the final degree of "degassing" ranges between ~35 and 70%. Those models were run for a notional 4 Ga, which would correspond to only about the first 0.4 Ga of Earth time in the present models (Fig. 2). The present results are roughly consistent with those of van Keken and Ballantine because the models are 60 to 80% processed within the first 0.4 Ga (Fig. 5).

The plausibility of the large degree of processing found in the present models can also be readily demonstrated in retrospect by using the following simple estimate. The rate at which mass passes through the midocean ridge melting zones is $\phi = \rho dLv$, where ρ is upper mantle density, d is the depth of the melting zone, L is the length of midocean ridges, and v is the average spreading rate of ridges. If the fraction of the mantle that remains unprocessed (i.e., primitive) at any given time is p, then the average rate at which primitive mantle is processed will be $p\phi$. Then the rate of change of p is given by

Fig. 9. Tracer characteristics from model Deepmelt (Fig. 8). (a) Age histograms for the MORB sample (solid lines) and OIB sample (dashed lines). (b) Tracer concentration. (c) Average ages. Profiles in (b) and (c) are shown at two times: 4.10 Ga (gray) and 4.44 Ga (black).

$$\frac{dp}{dt} = -\frac{p\phi}{M} = -p\tau \quad (4)$$

where M is the mass of the mantle and τ is a timescale defined by the second equality in Eqn. 4. τ is the time it would take to process the whole mantle at present rates of overturn. Eqn. 4 can be integrated to yield

$$p = e^{-t/\tau} \quad (5)$$

In other words, the fraction of primitive mantle remaining at any given time should decrease approximately exponentially with time, assuming the rate of processing through melting zones is approximately constant. Because we have already estimated that the amount of overturning the mantle has experienced is equivalent to 18 Ga of overturning at its present rate, we can estimate how much primitive mantle should remain. Taking ρ = 3300 kg/m^3, d = 100 km, L = 40000 km, and v = 100 mm/a, we get ϕ = 1.3×10^{15} kg/a. The mass of the mantle is ~4×10^{24} kg (Stacey, 1992), so the timescale τ is ~3 Ga. After 18 Ga, Eqn. 5 then yields p = 0.0025. In other words, only 0.25% of the mantle would remain primitive. There is some uncertainty in this result. For example, if the spreading rate is reduced to 50 mm/a, then τ = 6 Ga and 5% of the mantle would remain primitive. On the other hand, if the depth of melting is taken as 140 km, a value that might be more appropriate through the early part of Earth history when most of the processing occurs, then τ = 4.2 Ga and the present primitive fraction reduces again to 1.4%. Thus, these estimates are quite consistent with the results from the numerical models: no more than a few percent of the mantle is likely to be still primitive, and perhaps as little as a fraction of 1%.

The present results are more compatible than previous studies with such important observations as the lack of clear evidence for primitive isotopic signatures of refractory elements (Hofmann, 1997), evidence that the mantle has been strongly degassed of radiogenic noble gases (e.g., McDougall and Honda, 1998), and arguments that the mantle concentration of helium is at least two orders of magnitude lower than estimates of its initial concentration (Harper and Jacobsen, 1996).

5.3. Comparison of MORB and OIB Ages

Lead isotopes indicate that MORB and OIBs have similar mean apparent ages of ~1.8 Ga (Hofmann, 1997). The main difference between MORBs and OIBs is that the OIB ages are more scattered, perhaps even ranging from ~1 to ~2.7 Ga according to the early estimates of Chase (1981). The present models reproduce these relative characteristics. The model MORB and OIB ages are comparable, although the OIB ages span a larger range (Table 3). Also, greater variability of OIB ages with time is indicated by a tendency to greater variability of age variations with depth in Figures 4c and 9c. This variability should not be taken as more than an indication at this stage, however, because it is sensitive to the volumes of fluid averaged in the model sample, and the corresponding volume of deep mantle ultimately being sampled in OIBs is not at all well constrained at present.

One result from these models that is clear and significant is that the model OIB age is sensitive to the efficiency with which heavy tracers segregate into pools at the bottom. From Table 3,

the OIB age from model Dense100 is 28% greater and from model Deepmelt 17% greater, respectively, than the MORB age, whereas for the model Passive, the OIB age is 9% less. The reason for this effect is simply that heavier tracers are trapped for longer periods in the pools at the bottom of the model, as was reported by Christensen and Hofmann (1994). This effect provides a potentially important constraint on the efficiency of segregation in the mantle.

A significant implication of the present results is that only a small fraction of the denser material need accumulate at the base of the mantle to explain the apparent ages of MORBs and OIBs, even less than inferred by Christensen and Hofmann (1994), and so there is no requirement for the kind of thick layer postulated by Kellogg and others (Kellogg et al., 1999; van der Hilst and Kárason, 1999). Serious improvement on these estimates will depend on the slowly improving estimates of the relative densities of deep mantle phase assemblages.

5.4. Differences in Trace Element Concentrations between MORB and OIB

Models in which the tracers are heavy consistently yield a lower concentration of tracers at the top of the model than at the bottom, although the magnitude of the difference is quite sensitive to the parameters of the model. This results both from the accumulation of tracers at the base of the model and from settling of tracers through the upper mantle. The tracer concentration in the uppermost fluid is reduced by ~15 to 40%. The horizontally averaged tracer concentration increases by factors of 2 to 4 at the bottom of the two models with heavy tracers. However, these cases may more extreme than is plausible for the mantle.

The original hypothesis of Hofmann and White (1982) was that the geochemical differences between MORBs and OIBs could be explained if OIB sources contain a higher proportion of recycled ancient oceanic crust than does the MORB source. The trace element evidence can be accounted for (Hofmann, 1997) and the melting characteristics of plumes can correspond with flood basalt volumes (Leitch and Davies, 2001) if the OIB source contains 10 to 15% of additional oceanic crust. Because the basaltic component of the mantle is assumed here to correspond to ~10% of the mantle, this implies that the proportion of basaltic component is roughly doubled in the OIB source. This is readily achieved locally in these models (the local concentrations in pools and rising columns being implicitly higher than the horizontal averages reported in the figures). These results thus clearly support the hypothesis of Hofmann and White (1982), and the conclusion of Christensen and Hofmann (1994), with the additional suggestion that a significant part of the relative depletion of the MORB source might be due to settling within the upper mantle.

5.5. Tracer Segregation Mechanisms

The mechanisms by which tracers segregate may not be obvious from the still images shown here, especially to those not familiar with this kind of highly viscous flow. Movies are more revealing, and movies of the models Passive and Deepmelt can be viewed in the Electronic Supplement. However,

much of the following can be discerned from careful examination of Figures 6 and 8.

There is no significant segregation as lithosphere initially descends through the mantle (Fig. 8a), largely because the lithosphere is still cool and stiff. Once lithosphere has begun to warm, it often deforms by shortening and thickening (Fig. 8a, right) and sometimes also by buckling (Fig. 8a, center). Both kinds of deformation can yield quite large volumes of tracer-depleted fluid (see also Fig. 6a, lower left). Tracers will also be concentrated by these processes, although this is not readily discernible in the figures because the oceanic crust initially occupies such a small thickness. Once large, distinct volumes or strong concentrations have formed, buoyancy differences can operate at significant rates. In the lower mantle, the rates of rising or sinking are relatively slow, and the plate-scale circulation evidently prevents significant segregation in the body of the fluid, though not near the base of the fluid. However, in the upper mantle, where the viscosities are a factor of 30 smaller, the segregation rates are quite rapid. In fact the segregation can operate at relatively small scales. Because of this, large buoyant volumes that rise from the lower mantle are unstable, and break into smaller rising diapirs. Evidence of such breakup can be seen in Figure 8a.

The physics underlying these behaviors can be inferred from the theory of the motion of a buoyant sphere, which predicts that the sphere's ascent velocity is proportional to its density deficit, to its radius squared and to the inverse of the viscosity of the surrounding fluid (Batchelor, 1967; Davies, 1999a). For a given density difference, segregation is favored by large radius and by lower viscosity. Thus, it is the larger volumes in the lower mantle that show some evidence of buoyant segregation. In the upper mantle both large and medium-sized volumes can segregate. A greater local concentration of tracers will also favor segregation because this implies a greater mean local density difference.

A different process may be involved in the accumulation of tracers at the base of the model. The vertical velocity of the plate-scale flow necessarily approaches zero as the lower boundary is approached. This limits the ability of the large-scale flow to entrain tracers that happen to pass close to the lower boundary. Thus, sedimentation is enhanced close to the lower boundary. This mechanism has been demonstrated in laboratory models of crystal settling in magma chambers by Martin and Nokes (1989).

Christensen and Hofmann (1994) concluded that the segregation of heavy tracers occurred mainly in the bottom thermal boundary layer of their models, where the lithosphere would be warmed and softened, but that inference was already questioned in the Introduction. Because there is no hot thermal boundary layer at all in the present models (there is no heat entering through the base), this cannot be the mechanism of segregation here.

5.6. Seismic Tomographic Images

An argument advanced by van der Hilst and Kárason (1999) in favor of a distinct compositional layer in the deep mantle is that there is a distinct change in the character of tomographic images of the mantle in the bottom 1000 km or so: lateral variations do not correlate well with shallower patterns, and there are few examples of subducted lithosphere traceable below this depth.

Yet the structures predicted for the present Earth by the above models suggest a comparable change of character. This is most evident in Fig. 3d, which shows that the thermal expression of subducted material is less distinct in the deeper zone and, more importantly, buckling becomes predominant in the bottom third of the model. The buckling is due to the accumulation of cooler and therefore higher-viscosity material, combined with the residual stiffness of the sinking sheet (Fig. 1). This accumulated material spreads laterally and thus produces a significant change across the lower part of the model. It would be interesting to compute the expected tomographic effects of some of the models presented here, taking account of both thermal and compositional effects.

5.7. Consistency of Viscosity with Observational Constraints

It will be important to check whether the deep, high-viscosity regions predicted by these models are consistent with observational constraints. Viscosities in the deepest mantle are not very well constrained by postglacial and rotational observations, which tend to have poor resolution as well (Mitrovica, 1996; Lambeck and Johnston, 1998). It is therefore not implausible that the structures predicted here would not have been resolved. An additional consideration is that intervening lower-viscosity regions may dominate the large-scale response of the Earth, in the same way that lumps in oatmeal do not prevent the oatmeal from flowing, so long as there are not too many lumps.

6. REMAINING ISSUES

The persistence in the mantle of heterogeneities in the isotopic composition of refractory incompatible elements has been a long-standing puzzle, and the models presented here account for this persistence so readily that they leave room for adjustments and trade-offs of several parameters. The models also readily account for the depletion of basaltic component in MORB relative to OIB, as already demonstrated by Christensen and Hofmann (1994), and for the lack of a clear signature of primitive material. This type of model therefore would seem to provide a promising basis from which to explore other important geochemical characteristics of the mantle.

The noble gases provide another extensive set of observations of the mantle. A primary observation, that the MORB source has been strongly degassed (Allegre et al., 1987), is readily accounted for by these models. The inference that the lower mantle has been much less degassed would be inconsistent with these models, but this inference has recently come under serious question (Davies, 1999b; Honda and Patterson, 1999). An alternative interpretation of the available observations is that noble gas concentrations in OIB sources are no more than an order of magnitude greater than in the MORB source, and this difference could probably be accommodated in the type of model presented here. As mentioned earlier, there are peculiarities especially in the helium and argon data that are puzzling no matter what model one prefers for where they are accommodated in the mantle (Ozima, 1994; Albarède, 1998; Honda and Patterson, 1999). This indicates that processes have

operated on these gases that have not yet been clearly identified, and so the interpretation of the noble gas observations will require further elucidation.

Although the smaller scatter in MORB isotopic ratios compared with those in OIBs has been much discussed, it seems that it may tell us as much or more about the melting and magma ascent processes as about the degrees of heterogeneity that exist in the respective sources. Given the potential complexity of melting a heterogeneous mantle source and the emerging complexity of the melt migration and reaction problem (Aharonov et al., 1997; Spiegelman et al., 2001), it may be difficult to see through these processes to infer the degree of source heterogeneity, at least for some time to come. Therefore, the scatter of isotopic data does not seem to be a promising source of insights at present.

The question of how to accommodate the mass balances of trace elements between the atmosphere, the continental crust and the mantle is an important one whose reconciliation with this type of model is not trivial. The heat budget of the mantle is an important aspect of these balances, involving U, Th, and K in particular. These questions will be taken up in a separate article.

The nature of the tectonic regime that was operating in the Archean remains unclear (Davies, 1999a), and therefore, so does the nature of the main differentiations between the mantle and the whatever kinds of crust were forming at the time. It is clear that there were some major differences in tectonic style and geochemical signatures between the Archean and subsequent eras (Taylor and McLennan, 1985; Zegers and van Keken, 2001). Therefore, the presumption in these models that plate tectonics operated throughout their history is merely a convenient starting point. Although some alternatives have been explored briefly here, understanding of the ancient mantle will depend on improved understanding of the more accessible remnants of the ancient Earth (Davies and Richards, 1992; Richards and Griffiths, 1989; van der Hilst et al., 1997; van der Hilst and Kárason, 1999).

Associate editor: B. Mysen

REFERENCES

Aharonov E., Spiegelman M., and Kelemen P. (1997) Three-dimensional flow and reaction in porous media: Implications for the Earth's mantle and sedimentary basins. *J. Geophys. Res.* **102,** 14821–14834.

Albarède F. (1998) Time-dependent models of U-Th-He and K-Ar evolution and the layering of mantle convection. *Chem. Geol.* **145,** 413–429.

Albarède F. and van der Hilst R. D. (1999) New mantle convection model may reconcile conflicting evidence. *Eos, Trans. Am. Geophys. Union* **80,** 535.

Allegre C. J. and Turcotte D. L. (1985) Geodynamic mixing in the mesosphere boundary layer and the origin of oceanic islands. *Geophys. Res. Lett.* **12,** 207–210.

Allegre C. J., Staudacher T., and Sarda P. (1987) Rare gas systematics: Formation of the atmosphere, evolution and structure of the Earth's mantle. *Earth. Planet. Sci. Lett.* **81,** 127–150.

Batchelor G. K. (1967) An Introduction to Fluid Dynamics. Cambridge University Press.

Blankenbach B., Busse F., Christensen U., Cserepes L., Gunkel D., Hansen U., Harder H., Jarvis G., Koch M., Marquart G., Moore D., Olsen P., Schmeling H., and Schnaubelt T. (1989) A benchmark comparison for mantle convection codes. *Geophys. J. Int.* **98,** 23–38.

Campbell I. H. (1998) The mantle's chemical structure: Insights from the melting products of mantle plumes. In *The Earth's Mantle: Composition, Structure and Evolution* (ed. I. N. S Jackson), pp. 259–310. Cambridge University Press.

Campbell I. H. and Griffiths R. W. (1992) The changing nature of mantle hotspots through time: Implications for the chemical evolution of the mantle. *J. Geol.* **92,** 497–523.

Chase C. G. (1981) Oceanic island Pb: Two-stage histories and mantle evolution. *Earth Planet. Sci. Lett.* **52,** 277–284.

Christensen U. R. (1989) Mixing by time-dependent convection. *Earth Planet. Sci. Lett.* **95,** 382–394.

Christensen U. R. (1990) Reply to comment on "Mixing by time-dependent convection." *Earth Planet Sci. Lett.* **98,** 408–410.

Christensen U. R. (1996) The influence of trench migration on slab penetration into the lower mantle. *Earth Planet. Sci. Lett.* **140,** 27–39.

Christensen U. R. and Hofmann A. W. (1994) Segregation of subducted oceanic crust in the convecting mantle. *J. Geophys. Res.* **99,** 19867–19884.

Coltice N. and Ricard Y. (1999) Geochemical observations and one layer mantle convection. *Earth Planet. Sci. Lett.* **174,** 125–137.

Davies G. F. (1988) Ocean bathymetry and mantle convection, 1. Large-scale flow and hotspots. *J. Geophys. Res.* **93,** 10467–10480.

Davies G. F. (1990a) Comment on "Mixing by time-dependent convection" by U. Christensen. *Earth Planet. Sci. Lett.* **98,** 405–407.

Davies G. F. (1990b) Mantle plumes, mantle stirring and hotspot chemistry. *Earth Planet Sci. Lett.* **99,** 94–109.

Davies G. F. (1992) On the emergence of plate tectonics. *Geology* **20,** 963–966.

Davies G. F. (1995) Penetration of plates and plumes through the mantle transition zone. *Earth Planet. Sci. Lett.* **133,** 507–516.

Davies G. F. (1999a) Dynamic Earth: Plates, Plumes and Mantle Convection.Cambridge University Press.

Davies G. F. (1999b) Geophysically constrained mantle mass flows and the ⁴⁰Ar budget: A degassed lower mantle? *Earth Planet. Sci. Lett.* **166,** 149–162.

Davies G. F. and Richards M. A. (1992) Mantle convection. *J. Geol.* **100,** 151–206.

Farley K. A. and Neroda E. (1998) Noble gases in the Earth's mantle. *Annu. Rev. Earth. Planet. Sci.* **26,** 189–218.

Grand S. P. (1994) Mantle shear structure beneath the Americas and surrounding oceans. *J. Geophys. Res.* **99,** 11591–11621.

Grand S., van der Hilst R. D., and Widiyantoro S. (1997) Global seismic tomography: A snapshot of convection in the Earth. *Geol. Soc. Am. Today* **7,** (4) 1–7.

Griffiths R. W. and Campbell I. H. (1990) Stirring and structure in mantle plumes. *Earth Planet. Sci. Lett.* **99,** 66–78.

Griffiths R. W. and Richards M. A. (1989) The adjustment of mantle plumes to changes in plate motion. *Geophys. Res. Lett.* **16,** 437–440.

Gurnis M. and Davies G. F. (1986a) The effect of depth-dependent viscosity on convective mixing in the mantle and the possible survival of primitive mantle. *Geophys. Res. Lett.* **13,** 541–544.

Gurnis M. and Davies G. F. (1986b) Mixing in numerical models of mantle convection incorporating plate kinematics. *J. Geophys. Res.* **91,** 6375–6395.

Hager B. H. (1984) Subducted slabs and the geoid: Constraints on mantle rheology and flow. *J. Geophys. Res.* **89,** 6003–6015.

Harper C. L. and Jacobsen S. B. (1996) Noble gases and Earth's accretion. *Science* **273,** 1814–1818.

Hoffman N. R. A. and McKenzie D. P. (1985) The destruction of chemical heterogeneities by differential fluid motions during mantle convection. *Geophys. J. R. Astr. Soc.* **82,** 163–206.

Hofmann A. W. (1997) Mantle chemistry: The message from oceanic volcanism. *Nature* **385,** 219–229.

Hofmann A. W. and White W. M. (1982) Mantle plumes from ancient oceanic crust. *Earth Planet. Sci. Lett.* **57,** 421–436.

Honda M. and Patterson D. B. (1999) Systematic elemental fractionation of mantle-derived helium, neon, and argon in mid-oceanic ridge glasses. *Geochim. Cosmochim. Acta* **63,** 2863–2874.

Hunt D. L. and Kellogg L. H. (2001) Quantifying mixing and age variations of heterogeneities in models of mantle convection: Role of depth-dependent viscosity. *J. Geophys. Res.* **106,** 6747–6759.

Irifune T. and Ringwood A. E. (1993) Phase transformations in subducted oceanic crust and buoyancy relationships at depths of 600–800 km in the mantle. *Earth Planet. Sci. Lett.* **117,** 101–110.

Jacobsen S. B. and Wasserburg G. J. (1979) The mean age of mantle and crustal reservoirs. *J. Geophys. Res.* **84,** 7411–7427.

Karato S. and Wu P. (1993) Rheology of the upper mantle: A synthesis. *Science* **260,** 771–778.

Kellogg L. H. and Turcotte D. L. (1986) Homogenization of the mantle by convective mixing and diffusion. *Earth Planet. Sci. Lett.* **81,** 371–378.

Kellogg L. H. and Turcotte D. L. (1990) Mixing and the distribution of heterogeneities in a chaotically convecting mantle. *J. Geophys. Res.* **95,** 421–432.

Kellogg L. H., Hager B. H., and van der Hilst R. D. (1999) Compositional stratification in the deep mantle. *Science* **283,** 1881–1884.

Kesson S. E., Fitz Gerald J. D., and Shelley J. M. G. (1994) Mineral chemistry and density of subducted basaltic crust at lower mantle pressures. *Nature* **372,** 767–769.

Kesson S. E., Fitz Gerald J. D., and Shelley J. M. (1998) Mineralogy and dynamics of a pyrolite lower mantle. *Nature* **393,** 252–255.

Lambeck K., Johnston P. (1998) The viscosity of the mantle: Evidence from analyses of glacial rebound phenomena. In *The Earth's Mantle: Composition, Structure and Evolution* (ed. I. N. S. Jackson), pp. 461–502. Cambridge University Press.

Leitch A. M. and Davies G. F. (2001) Mantle plumes from flood basalts: Enhanced melting from plume ascent and an eclogite component. *J. Geophys. Res.* **106,** 2047–2059.

Martin D. and Nokes R. I. (1989) A fluid-dynamical study of crystal settling in convecting magmas. *J. Petrol.* **30,** 1471–1500.

McDougall I., Honda M. (1998) Primordial solar noble-gas component in the Earth: Consequences for the origin and evolution of the Earth and its atmosphere. In *The Earth's Mantle: Composition, Structure and Evolution* (ed. I. N. S. Jackson), pp. 159–187. Cambridge University Press.

McKenzie D. P. and Bickle M. J. (1988) The volume and composition of melt generated by extension of the lithosphere. *J. Petrol.* **29,** 625–679.

Mitrovica J. X. (1996) Haskell [1935] revisited. *J. Geophys. Res.* **101,** 555–569.

O'Nions R. K. and Tolstikhin I. N. (1996) Limits on the mass flux between the lower and upper mantle and stability of layering. *Earth Planet. Sci. Lett.* **139,** 213–222.

Ozima M. (1994) Noble gas state in the mantle. *Rev. Geophys.* **32,** 405–426.

Richards M. A. and Griffiths R. W. (1989) Thermal entrainment by deflected mantle plumes. *Nature* **342,** 900–902.

Sleep N. H. (1990) Hotspots and mantle plumes: Some phenomenology. *J. Geophys. Res.* **95,** 6715–6736.

Spiegelman M., Kelemen P. B., and Aharonov E. (2001) Causes and consequences of flow organization during melt transport: The reaction infiltration instability in compactible media. *J. Geophys. Res.* **106,** 2061–2078.

Stacey F. D. (1992) Physics of the Earth. Brookfield Press.

Taylor S. R., McLennan S. M. (1985) The Continental Crust: Its Composition and Evolution. Blackwell.

van der Hilst R. D., Widiyantoro S., and Engdahl E. R. (1997) Evidence for deep mantle circulation from global tomography. *Nature* **386,** 578–584.

van der Hilst R. D. and Kárason K. (1999) Compositional heterogeneity in the bottom 1000 km of Earth's mantle: Towards a hybrid convection model. *Science* **283,** 1885–1888.

van Keken P. E. and Ballantine C. J. (1998) Whole-mantle versus layered-mantle convection and the role of a high-viscosity lower mantle in terrestrial volatile evolution. *Earth Planet. Sci. Lett.* **156,** 19–32.

van Keken P. E. and Ballantine C. J. (1999) Dynamical models of mantle volatile evolution and the role of phase transitions and temperature-dependent rheology. *J. Geophys. Res.* **104,** 7137–7151.

Zegers T. E. and ven Keken P. E. (2001) Middle Archean continent formation by crustal delamination. *Geology* **29,** 1083–1086.

Zindler A. and Hart S. (1986) Chemical geodynamics. *Ann. Rev. Earth Planet. Sci.* **14,** 493–570.